Evolution of random directional wave and rogue wave occurrence

Takuji Waseda[1]
Department of Environmental & Ocean Engineering, the Univ. of Tokyo
7-3-1 Hongo, Bunkyo-ku, Tokyo 113-8656, JAPAN
e-mail: waseda@naoe.t.u-tokyo.ac.jp tel: +81-3-5841-6540

Takeshi Kinoshita
Institute of Industrial Science, the University of Tokyo
4-6-1 Komaba, Meguro-ku, Tokyo 153-8505, JAPAN
e-mail: kinoshit@iis.u-tokyo.ac.jp tel : +81-3-5452-6170

Hitoshi Tamura
[1]Frontier Research Center for Global Change/JAMSTEC
3173-25 Showamachi, Kanazawa-ku, Yokohama, Kanagawa 236-0001, JAPAN
e-mail: htamura@jamstec.go.jp tel: +81-45-778-5519

ABSTRACT
The probability of extreme waves exceeding twice the significant wave height (i.e. the rogue waves), is suggested to be a function of wave steepness and frequency bandwidth. The combined parameter is named the "Benjamin-Feir" index suggesting that the non-resonant wave-wave interaction (or the Benjamin-Feir instability in some cases) is responsible for the increased rogue wave occurrence. However, recent studies suggest that the non-resonant wave-wave interaction is suppressed by the directionality of the wave spectrum. Preliminary study suggested that for a given steepness and frequency bandwidth, the Kurtosis (and hence the probability of the rogue wave) rapidly decreases as the spectrum broadens (Waseda, 9th Wave WS). In this report, we will present results from the additional experiment conducted using the directional wave maker located at one end of a rectangular basin (50m long, 10 m wide, 5 m deep, Kinoshita lab IIS). The experimental parameters cover ranges of directional spreading (unidirectional to broad), steepness, and frequency bandwidth with a conventional JONSWAP-Mitsuyasu type spectrum. Other directional distributions such as the observed one by Hwang & Wang (2001) and bimodal distribution were studied as well. The results will be discussed isolating effects of strong nonlinearity (i.e. wave breaking), relative significance of bound waves and instability, and effects of discretization of the spectrum. In particular, the spectral downshifting due to wave breaking plays an important role in the increase of the Kurtosis. Implication of these findings to the rogue wave prediction utilizing 3rd generation wave models will be discussed as well.

1. INTRODUCTION
At the University of Tokyo, we have been conducting a research project since 2004, together with the National Maritime Research Institute, to understand the generation mechanism of freak/rogue wave and its impact on ships, and to establish a prediction and avoidance system of extreme waves near Japan. The joint effort includes wave tank experiment, numerical simulation and radar/buoy observation. At JAMSTEC, the first and the third author has been working towards establishment of an operational wave-current coupled model as an extension to the Japan Coastal Ocean Prediction Experiment (JCOPE, Tamura et al. R1 10th Wave WS). We report here, the results from the recent tank experiment and a brief discussion that utilizes the results from the Wave-JCOPE hindcast run.

The working hypothesis of the current study is the following: first waves in the ocean evolve under the influence of the meteorological conditions and wave-current interaction (dispersive and geometric focusing); next, when the resulting wave spectrum satisfies certain condition, the wave system becomes unstable and the non-resonant interaction kicks in. The latter process has been studied by numerous authors (Janssen 2003, Onorato et al. 2004, Mori and Janssen 2006) and was shown both theoretically and experimentally that for uni-directional

wave system the significance of the non-resonant interaction can be measured by the magnitude of a single index called the BFI which is the ratio of the steepness and the frequency bandwidth. Other works have suggested that when directionality is included (Soquet-Juglard et al. 2005, Onorato et al. 2002) the effect of non-resonant interaction diminishes.

At the 9th International Workshop on Wave Hindcasting and Forecasting, preliminary analyses of the evolution of random directional wave, as observed in a laboratory wave tank, were presented. There, we have suggested that the directional spreading will weaken the effect of non-resonant interaction; i.e. the Kurtosis reduces with directional spread. The result drew attention of those who were conducting similar studies under the frame-work of weak nonlinearity. However, the first set of experiments was strongly affected by the presence of energetic breakers. To extend the work, the authors have repeated the experiment with a better control of wave maker and thereby covered waves with none or relatively less frequent wave breakers. We present here the results from the newly conducted experiments with minimum influence of breaking dissipation.

Since the non-resonant interaction plays a key role in the evolution of narrow random directional wave, we first review studies of the evolution of Benjamin-Feir instability and the long-term evolution of the modulational wave train that follows (section 2, background). In section 3, the tank experiment will be described in detail. The control of the wave generator, observed cross-tank variability of the wave records and some assessment of the effects of narrow flume will be discussed. In section 4, we present main results from the two experiments conducted in August 2006 and in April 2007. This section will address issues of the higher order statistics (the Kurtosis), spectral downshifting due to breaking dissipation, and maximum wave height. Finally, in section 5 the possible implication of the experimental finding will be discussed including analyses of the high-resolution wave-current coupled model.

2. BACKGROUND

Occurrence of freak waves in the ocean is not well understood and many researches have been seeked the answer in the framework of the weakly nonlinear theory for a narrow banded wave system. The evolution of such waves can be described by the Nonlinear Schrodinger equation, and the use of NLS to represent the ocean wave dates back to the work by Yuen and Lake (1982). Extending the study of the unstable Stokes wave by Benjamin and Feir (1967), they have shown that the instability leads to the formation of wave group. In the 1990s, the evidence of wave group in the open ocean was provided by numerous low grazing angle radar observations (Poulter et al. 1994, Lamont-Smith et al. 2003, Tulin 2001). However, until recently when the interest in understanding the freak/rogue wave generation grew, the significance of such wave group formation in the ocean has been depreciated. The view has changed and many people now regard the non-resonant interaction is at work in the ocean. Formally the theory of the discrete wave system (Benjamin-Feir instability) was extended to describe the evolution of continuous directional wave system by Alber and Safman (1978), who have shown theoretically that the wave system is unstable only when the directional distribution is less than 35 degrees or so. The theory suggests that the wave group formation becomes significant only for a narrow spectrum. The non-resonant interaction is neglected in Hasselmann's four wave interaction theory (Hasselmann et al. 1985) and the Zakharov's equation (Zakharov 1968) should be used instead. Janssen (2003) has demonstrated the use of the Zakharov's equation in correcting the higher order statistic (i.e. the Kurtosis) of the uni-directional wave system. This led to the modification of the conventional Rayleigh distribution of the wave height to increase the occurrence of waves exceeding twice the significant wave height (Onorato et al. 2004, Mori and Janssen 2006). Of course, as Albers and Saffman have indicated, such mechanism is most effective for uni-directional wave system, and as Soquet-Juglard et al. (2005) and Onorato et al.

(2002) have indicated, the efficiency reduces with increased directionality. For a broad spectrum, the Hasselman's four wave interaction (i.e. the resonant interaction) is most efficient in transferring energy among wave components.

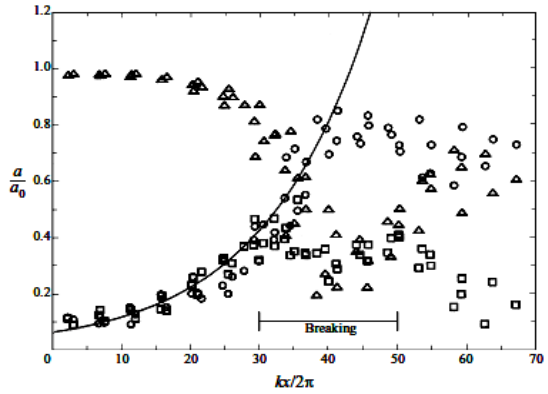

Fig.1 Evolution of wave amplitudes of the three wave system; triangle: carrier wave; circle: lower sideband; square: upper sideband. Permanent downshifting occurs after the breaking event.

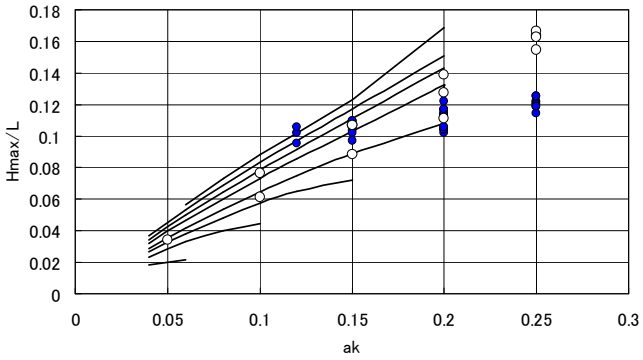

Fig.2 Maximum wave height of the unstable Stokes wave, plotted against initial steepness. Solid circle: Experiment; open circle: from Zakharov equation solutions; lines: from Dysthe's equation solutions

The freak wave, therefore, may not be an abnormal wave for a normal wave condition when Hasselman's four wave interaction is dominant. Rather, we can hypothesize that *the freak wave is an expected wave in an abnormal condition when the wave spectrum narrows and the non-resonant interaction becomes significant*. The extreme case is the unstable Stokes wave train whose evolution is well represented by an interaction of the carrier wave and the two perturbing side band waves. The three waves will not satisfy the exact resonance condition and when the resonance detuning and the amplitude dispersion cancel each other, the sideband waves grow exponentially. As the sideband waves become finite in amplitude, the linear approximation fails and the growth slows down. The long-term evolution will then go through the so-called Fermi-Pasta-Ulam recurrence which is a repetition of the growth of the sideband and their decay to return to its original state. The process becomes irreversible when the modulated wave breaks at the peak modulation and energy is lost from the system accordingly; see Fig.1 (Melville 1982, Waseda and Tulin 1999). The loss of energy is associated with the permanent downshifting of the spectral peak, which can then be accounted for by the balance of energy and momentum loss from the system (Waseda and Tulin 1999). In summary,

- Stokes wave is unstable to sideband perturbation and the evolution is followed by the formation of the wave group:
  - For case without breaking dissipation, wave system undergo recurrence
  - With energetic breakers, balance of energy and momentum loss leads to permanent downshifting of the spectrum

Then the following can be hypothesized for continuous directional spectrum:

- Resonant interaction is dominating for a broad spectrum
  - Spectrum downshifts due to resonance interaction
- Non-resonant interaction becomes significant as the directionality reduces
  - Without breaking dissipation, evolution becomes recursive and the wave spectrum remains unchanged
  - With energetic breaker, combination of instability and energy/momentum loss from the system leads to permanent downshifting of the spectrum

As hypothesized, we expect downshifting of the spectrum for spectrally narrow and energetic wave which should be confirmed experimentally.

So when will the wave break? From the previous work (Waseda et al. 2005), the maximum wave height of the unstable Stokes wave is given as a function of initial wave steepness (Figure 2). The maximum wave height was empirically determined from a parameter sweep experiment varying the initial wave steepness and the frequency bandwidth (or the sideband frequencies) in a laboratory wave tank. For a given initial steepness, the maximum wave height has a small scatter due to the difference in the sideband wave frequency. The scatter, however, is much less than the scatter of the maximum wave heights estimated based on the weakly nonlinear theory (solid lines, using Dysthe's 2D extended NLS equation), because the wave breaking imposes an upper limit to the achievable maximum wave height. We will extend this work to the continuous wave spectrum.

3. TANK EXPRIMENT

Experiment was conducted at a 50m long, 10 m wide, and 5 m deep wave tank of the Institute of Industrial Science, University of Tokyo (Kinoshita laboratory/Rheem laboratory). The segmented plunger type directional wave maker (32 plungers) is digitally controlled by arbitrary wave forms. In this study, we consider the directional wave spectrum in the following form:

$$N(\omega,\theta) = S(\omega)\cdot G(\theta;\omega) \tag{1}$$

The wave maker control signal can be constructed from any given frequency spectrum $S(\omega)$ and directional spreading function $G(\theta;\omega)$. The directional spectrum is discretized by energy conserving method and the directional wave can be generated by either single summation (SS) method or the double summation (DS) method. The former assigns single direction for each frequency component (1024 frequencies were used), considered the directional spreading function as a probability density function. SS method is used only for cases when the directional spreading function does not depend on frequency $G(\theta;\omega) \approx G(\theta)$. Thus the wave signal is constructed as a linear superposition of 1024 waves with random initial phases e_n;

$$\begin{cases} \eta(x,y,t) = \sum_{n=1}^{n=1024} a_n \cos(\omega_n t - \mathbf{k_n}\cdot\mathbf{x} + e_n) \\ a_n = \sqrt{2S(\omega_n)\Delta\omega} \end{cases} \tag{2}$$

The DS method assigns multiple directions for each frequency so the wave signal is given as,

$$\begin{cases} \eta(x,y,t) = \sum_{n=1}^{N}\sum_{m=1}^{M} a_{n,m} \cos(\omega_n t - \mathbf{k}_m\cdot\mathbf{x} + e_{n,m}) \\ a_{n,m} = \sqrt{2S(\omega_n)G(\theta_m;\omega_n)\Delta\omega\Delta\theta} \end{cases} \tag{3}$$

where $N\times M = 1024$, and typically N and M are order 10.

For all the experiments conducted, the frequency spectrum was kept to be of the JONSWAP type

$$S(f) = \alpha g^2 (2\pi)^{-4} f^{-5} \exp\left\{-\frac{5}{4}\left(\frac{f}{f_p}\right)^{-4}\right\}\gamma^{\exp\left\{\frac{(f-f_p)^2}{2\sigma^2 f^2 p}\right\}}, \tag{4}$$

The control parameters in this study were α, γ and n, that are closely related to the significant wave height, the frequency bandwidth, and the directional spread respectively. The wavelength at the spectral peak f_p is 1 meter so the tank length is approximately 50 wavelengths. The directional spreading function was selected among the Mitsuyasu-type,

$$G(\theta) = G_n \cos^n(\theta). \tag{5}$$

the Hwang type, and the Bimodal type. The Hwang type (Hwang and Wang 2001) is an empirical fit to the high resolution directional spectrum obtained by scanning Lidar in the open ocean and is characterized by the bimodal directional spreading at high frequency (Figure 3). The bimodal distribution was artificially created by selecting a section of the Hwang distribution at arbitrary frequency.

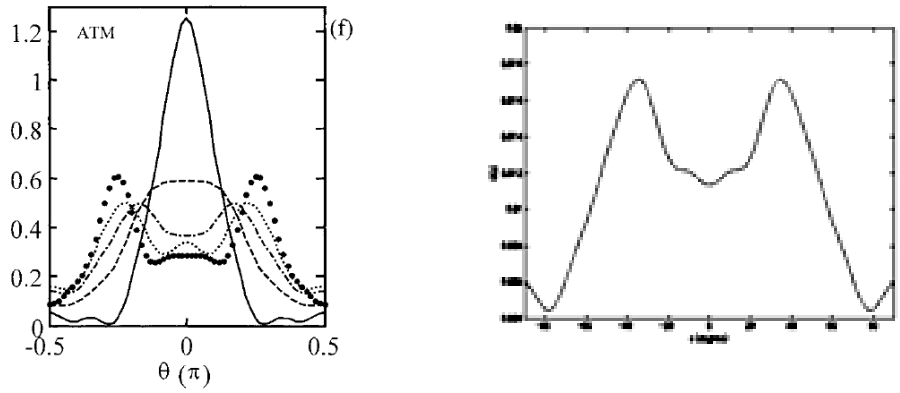

Figure 3: (Left) Hwang & Wang directional spreading function. (Right) Bimodal directional distribution

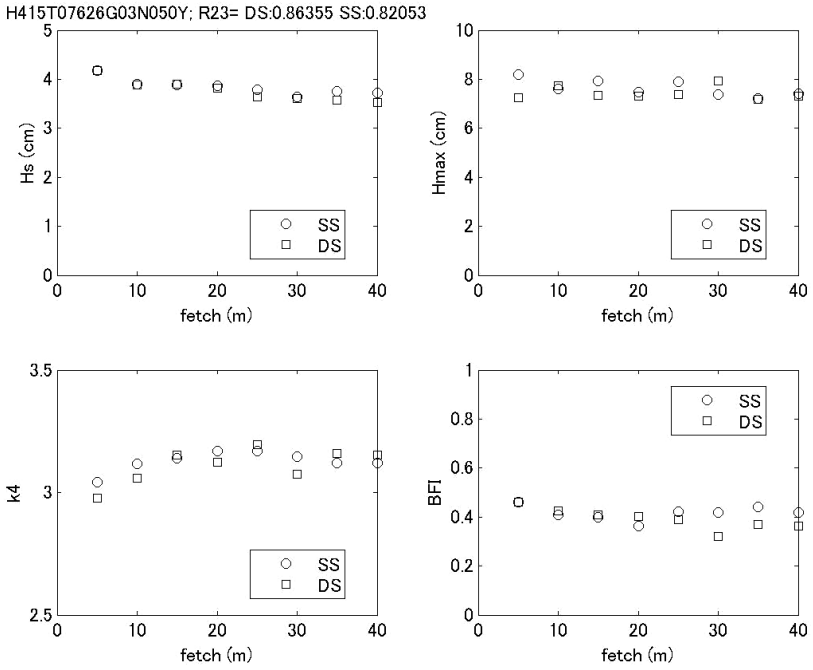

Figure 4: Comparison of DS and SS wave generation. Significant wave height, maximum wave height, kurtosis, and the BFI are compared for an identical directional wave spectrum (γ=3.0 and n=50), from an hour record.

The array of wave wires were arranged at 5 m intervals from 5 to 40 m from the wave maker, 2.6 m away from the side wall; four wave wires were arranged at 14 m at the center to estimate directional spectra. Two additional wave wires were located at 3.8 and 5 meters away from the side wall at fetch 15m as well. In figure 4, various wave parameters (which will be described later) from the wires along the sidewall, are compared between DS and SS methods. At first

glance, there seems to be no critical differences to be concerned. The significant wave height (upper left) is nearly identical. Other parameters, for example the maximum wave height, seem to show random variation between SS and DS method. The difference, however, is likely not just because of the difference in the wave generation methods (SS vs. DS). As seen in Figure 5, cross tank variation (measured at center, 1m and 2m from the center) is comparable to the variation between DS and SS generation. Within the 10 minutes record, the cross tank variation did not show any regular pattern.

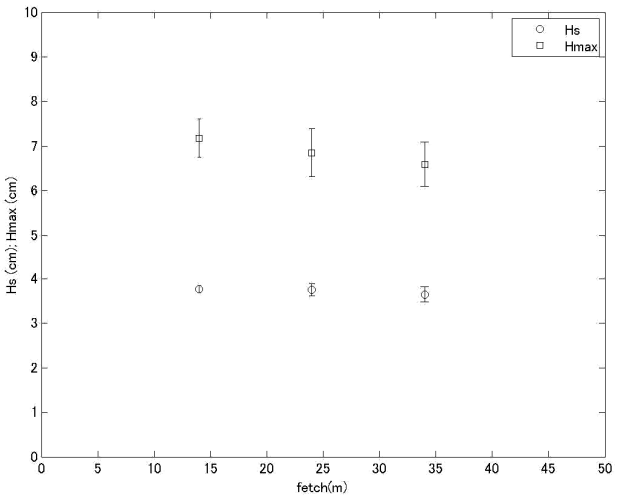

Figure 5: Cross tank variation of the significant wave height (circle) and the maximum wave height (square). The error bar is the standard deviation of the cross tank variation from 10 minutes record.

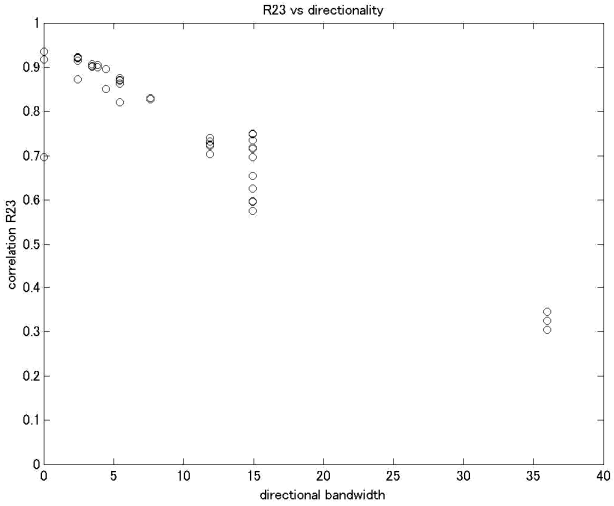

Figure 6: Cross correlation (32cm across tank) for all the cases. Note that except for the Hwang cases (at directional bandwidth 15) the correlation reduces with directional bandwidth.

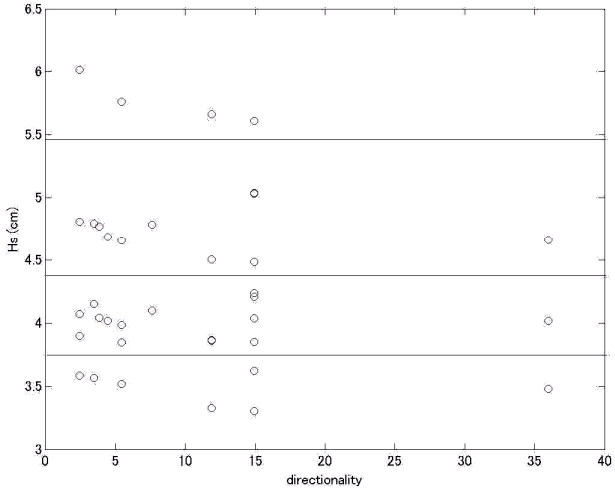

Figure 7: Summary of experimental parameters, significant wave height and directionality.

The directional spectra was estimated from the four wires at 14 m using Maximum Likelihood Method, Maximum Entropy Method and Wavelet Detection Method but none of the analysis was adequate in resolving the subtle changes of the directionality imposed by the wave generator. The cross correlation between two wires separated by 32 cm (at fetch 14m) was used

as an alternative indicator of the actual directional spreading (Figure 6). For most cases, as the imposed directional bandwidth[1] increases, the cross correlation reduces, suggesting that the correlation length scale reduced. The large scatter of data at 15 degrees directional bandwidth is caused by the Hwang directional distribution cases; apparently, the generated directional spreading varied because the directional spreading function was a function of frequency. The sets of significant wave heights selected in this study are displayed in Figure 7 plotted against the imposed directionality (not the actual directionality). The corresponding steepness ranged between 0.05 and 0.09 and those cases exceeding Hs=5.5 cm had an energetic breaker. The magnitude and frequency of the breaker decreased with reduction of Hs.

4. RESULTS

The random directional waves were successfully generated varying the steepness (as controlled by the significant wave height), directional spreading (as indicated by the cross correlation) and the frequency bandwidth. Since the wave generator signal was adjusted so that the frequency spectrum at fetch 14 m best matches the intended frequency spectrum, in the rest of the analyses, the 14m fetch is considered the initial condition. The developed stage is the average of 35 m fetch and 40 m fetch measurements.

4.1 Maximum wave height

The highest wave height in an unstable wave train was empirically determined by Su and Green (1984) and numerically by Tanaka (1990). Extensive experiments were conducted at the U. of Tokyo Ocean Engineering Tank varying the initial steepness and the sideband frequency and the results were compared against weakly nonlinear theory (Waseda 2006). The results suggested that for initial wave steepness over 0.11, the maximum wave height is limited by wave breaking. Thus the maximum wave height remains relatively unchanged and with increase of the initial steepness, the breaking strength increases accordingly. We now extend this study to continuous spectral case.

The initial steepness and the wavelength are defined as follow:

$$\begin{cases} ak \equiv \sqrt{2m_0}\,\dfrac{2\pi}{L_p} \\ L_p \equiv \dfrac{g}{2\pi}\left(1.05\,T_{1/3}\right)^2 \end{cases} \tag{7}$$

where m_0 is the variance of the surface elevation, L_p is the wavelength at spectral peak and $T_{1/3}$ is the significant wave period. The maximum wave height is determined from the entire wave record, which includes over 4000 waves (an hour record) sufficiently long enough to capture the so-called freak wave that exceeds twice the significant wave height. Figure 8 compares the normalized maximum wave height $H_{\max}/L_p$ against the wave steepness ak. The new result (open circle) tends to follow the upper limit of the maximum wave height curve estimated by the weakly nonlinear theory (Figure 2).

---

[1] The directional spreading factor w is defined as the angle where half of the wave energy is contained, $\frac{1}{2} = \int_{-w\pi}^{w\pi} (\cos\theta)^N \, d\theta \Big/ \int_{-\pi/2}^{\pi/2} (\cos\theta)^N \, d\theta$ and the corresponding directional spreading (directionality) is given as $w \times 180$ degrees. For other directional distributions, the integrant should be replaced accordingly.

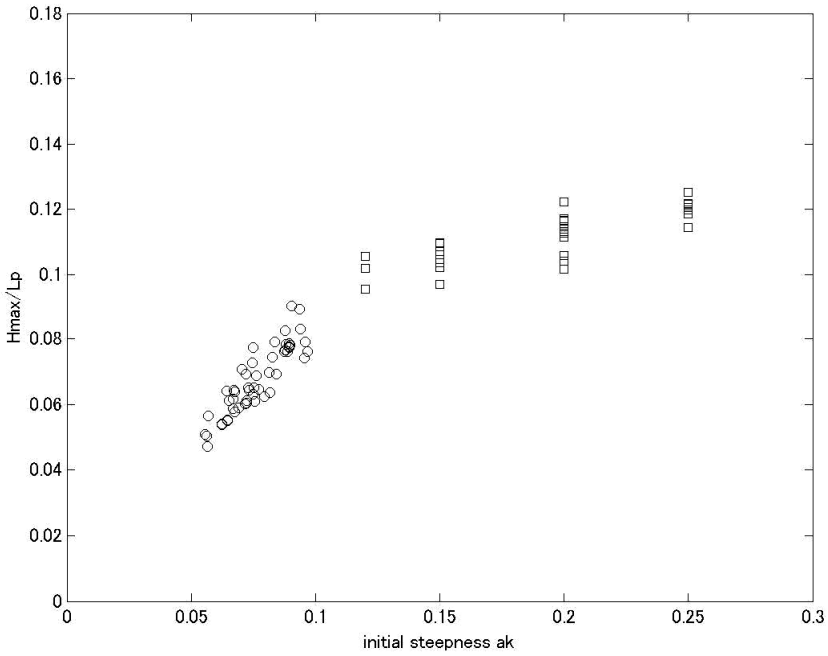

Figure 8: Normalized Maximum wave height $H_{\max}/L_p$ against wave steepness ak. The circle: the new experimental result of random directional wave; the square: earlier result from the Benjamin-Feir instability experiments.

The wave breaking was not apparent in most cases except for the case of large initial steepness where relatively strong breaker was observed. The data scatters because the experiments included various spectral bandwidths and directionality. Nevertheless, the variation of the maximum wave height due to directional spreading and frequency bandwidth is comparable to the variability of the uni-directional cases (i.e. the Benjamin-Feir instability or the 3 wave system), which suggests that a simple 3 wave system captures the main characteristics of the directional wave system. Theory of the 3 wave system suggests that the narrower the spectrum, the higher the maximum wave height as indicated by lines in Figure 2, which is consistent with visual observation of the directional waves. Since the highest wave height is closely related to the magnitude of the kurtosis, the dependency of the maximum wave height on frequency bandwidth and directionality will be revisited in section 4.3.

4.2 Spectral downshift

Typical spectral evolution is shown in Figure 9. The spectral parameters characterizing the shape of the directional spectrum are identical (γ=3.0and n=125) but the significant wave height differs (Hs=4 cm and 5 cm). Notable feature common in both cases is the downshifting of the spectral peak at its developed stage (40 m fetch) from the initial stage (15m fetch). Spectral downshifting is believed to be caused by the resonant four-wave interaction, and its magnitude depends on the spectral shape. The most efficient interaction occurs for a combination of waves that include two waves separated from the other two identical waves by 11.5 and -33.6 degrees (e.g. DIA, Hasselman et al 1985). Thus, when the wave spectrum becomes extremely narrow in direction, the resonance interaction becomes unimportant and the wave tends to disperse. This process is nothing but a transition from wind-waves to swell. The directional spreading of the spectrum shown in Figure 9, are about 7 degrees and should be considered as a swell. Then, downshifting due to resonant interaction is not likely to take place. However, both cases downshift and furthermore, comparison of the two cases suggests that the higher the initial steepness the faster the downshifting rate.

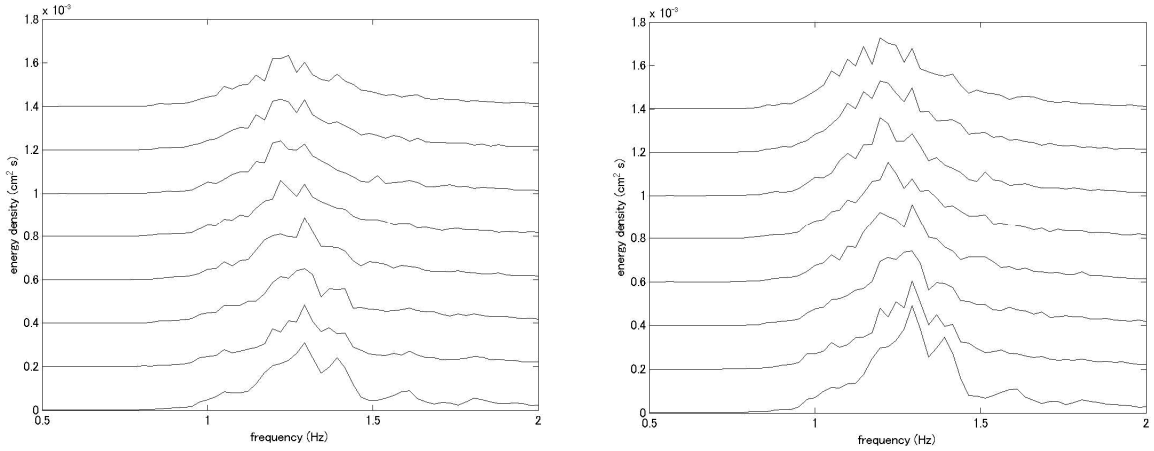

Figure 9: Spectral evolution at 5 m interval from 5 m to 40 m fetch (energy is artificially shifted). Left: γ=3.0 and n=125, Hs is about 4 cm (ak=0.06); Right: γ=3.0 and n=125, Hs is about 5 cm (ak=0.08)

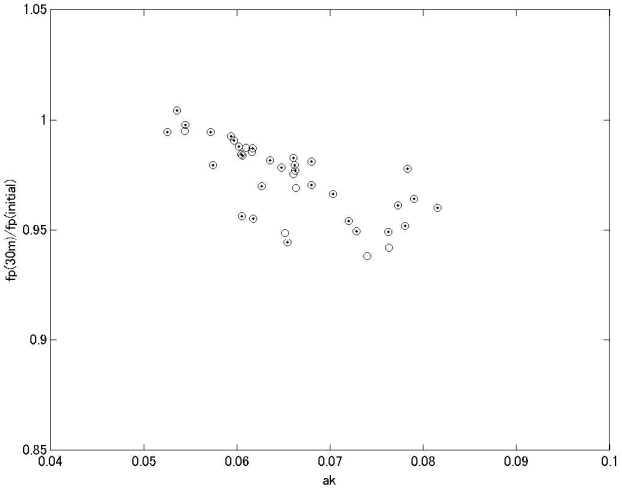

Figure 10: Frequency downshift plotted against initial steepness for all the cases.

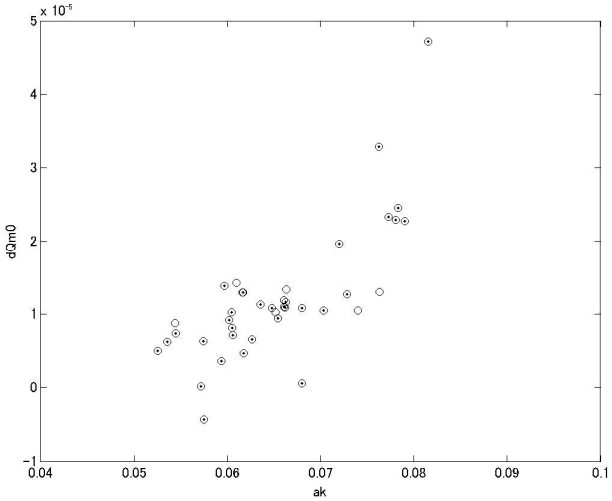

Figure 11: Energy loss plotted against initial steepness for all the cases.

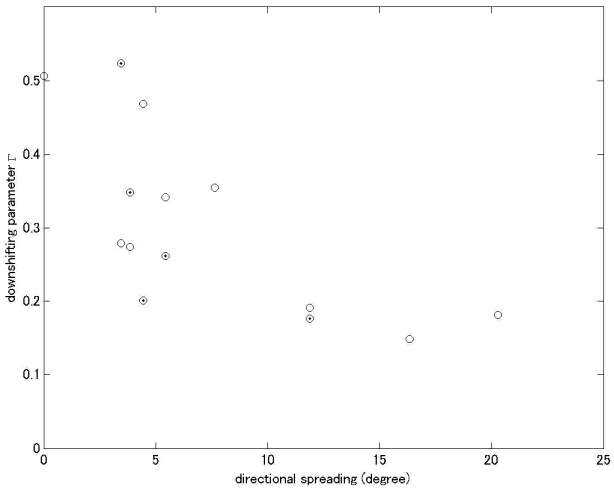

Figure 12: Downshifting parameter Γ against directional spreading (degree) for cases with energetic breakers

According to the four-wave interaction theory, it is not apparent why the downshifting rate should increase with steepness alone. In Figure 10, the spectral downshifting rate is summarized for all the experimental cases. Regardless of the directionality and frequency bandwidth, the downshifting magnitude, defined as the ratio of peak frequency at fetch 35-40 m (developed state) and that at fetch 10-15 m (initial state), the downshifting rate increases with steepness. The downshifting magnitude, on the other hand, is not a straightforward function of directionality and frequency bandwidth. From the study of the Benjamin-Feir instability, we know that the downshifting for a narrow banded system is related to the energy loss due to breaking dissipation. We have compared the energy loss (defined as the difference of rms elevation between the developed state and the initial state) against the steepness (Figure 11). An increasing tendency of the magnitude of the energy loss with the steepness is apparent. Breaking dissipation seems to govern the downshifting process, rather than the weakly nonlinear wave-wave interaction. To clarify, we analyze further the cases with energetic breakers.

Downshifting theory based on conservation of energy and momentum was first presented by Tulin and Waseda (1999). Here we briefly summarize their derivation and apply to the analysis of the current experimental result. We consider a set of free waves whose total energy E_T and momentum M_T are described as:

$$E_T = \sum_j E_j \qquad \text{and} \quad \dot{E}_T = -D_b$$
$$M_T = \sum_j M_j \quad \text{where} \quad E_j = c_j M_j = \frac{g}{\omega_j} M_j \tag{8}$$

Here, D_b is the energy loss due to dissipation, c is the celerity and ω is the angular frequency of each wave component where subscript j labels each wave component. The rate of change of the first moment of the angular frequency,

$$\omega_p = \frac{\sum_j \omega_j E_j}{\sum_j E_j} = \frac{\sum_j \omega_j E_j}{E_T} \tag{9}$$

can be readily derived as,

$$\frac{d\omega_p}{dt} = \frac{\omega_p}{E_T}\left(c_p \dot{M}_T - D_b\right) \approx -\frac{\omega_p}{E_T}\Gamma D_b \tag{10}$$

where the proportionality of $c_p \dot{M}_T$ and D_b was heuristically assumed. Therefore, the proportionality factor

$$\Gamma = \frac{d\omega_p}{dt}\frac{1}{\omega_p}\Big/\left(\frac{D_b}{E_T}\right) \equiv \frac{\text{rate of frequency downshift}}{\text{rate of energy loss}} \tag{11}$$

can only be determined empirically. Tulin and Waseda (1999) empirically determined that $\Gamma \approx 0.4$ for the case of an unstable Stokes wave.

We extended their work and estimated Γ for the random directional wave. First, the rate of frequency downshift $\left(d\omega_p/dt\right)/\omega_p = d\ln\omega_p/dt$ and rate of energy loss $D_b/E_T = d\ln E_T/dt$ were estimated by regression and then the value of Γ was obtained as the ratio of the estimated exponents. The result, Figure 12, suggests that the value of Γ for uni-directional case is similar to the value obtained by Tulin and Waseda, but tends to decrease as the directional bandwidth broadens. The value of the estimated Γ do not approach zero, suggesting that the energy loss and momentum loss cannot balance to equilibrate the spectrum.

4.3 Freak wave occurrence

In the previous section, cases with energetic breakers were analyzed. Diagnosis of the balance of energy and momentum loss suggested a driving mechanism for the evolution of a narrow banded wave system under strong nonlinearity. In this section, we limit the analysis to cases with minimum breaking, to highlight the impact of spectral broadness on the intensity of the non-resonance interaction. Following Onorato et al. (2005), the forth moment of the surface elevation can be expressed as a summation of linear Gaussian component, the correction term due to non-resonance interaction (free waves) and the correction due to the distortion of the wave shape (Stokes correction; bound waves)

$$\left\langle \eta(x)^4 \right\rangle = 3\left\langle \eta(x)^2 \right\rangle^2 + 16\int M_{1,2,3,4} T_{1,2,3,4} N_1 N_2 N_3 \frac{1-Cos(\Delta\omega t)}{\Delta\omega} \delta_{1+2-3-4} dk_{1234} + 12\int \mathrm{K}_{1,2,3,1,2,3} N_1 N_2 N_3 dk_{123} \tag{12}$$

The kurtosis $\kappa_4 \equiv \left\langle \eta^4 \right\rangle \Big/ \left\langle \eta^2 \right\rangle^2$ is 3 when the higher order terms can be ignored. The second term has been numerically studied for uni-directional case by Janssen (2003) and experimentally by Onorato et al. (2004). Figure 13 presents an example of the evolution of the kurtosis from our experiment for relatively small directional spread (γ=3.0, n=125).

Janssen (2003) have shown that the intensity of the second term at the developed state can be parameterized by the Benjamin-Feir Index:

$$\kappa_4 = 3.0 + \frac{\pi}{\sqrt{3}} BFI^2; \quad BFI = \frac{\sqrt{2}\varepsilon}{2\delta f / f_p} \tag{13}$$

where ε is the steepness and δf is the frequency bandwidth of the spectrum. The reader is reminded here that the inverse of the BFI is closely related to the growth rate of the sideband wave as derived by Benjamin and Feir (1967); $\beta = \varepsilon^2 \delta \left(2.0 - \delta^2\right)^{1/2}$ where $\delta = \left(\sqrt{2} \times \mathrm{BFI}\right)^{-1}$. When $\delta > \sqrt{2}$ ($BFI < 1$), the growth is suppressed. The improved growth rate based on the Zakharov's equation (e.g. Waseda and Tulin 1999) suggests that the wave train is unstable for $\delta < 1.2$ ($BFI > 0.58$). Note that the BFI from a spectrum is estimated following Janssen and Bidlot (2003):

$$BFI = k_0 m_0^{1/2} Q_p \sqrt{2\pi} \quad \text{where} \quad Q_p = 2/m_0^2 \int d\omega\, \omega E^2(\omega) \tag{14}$$

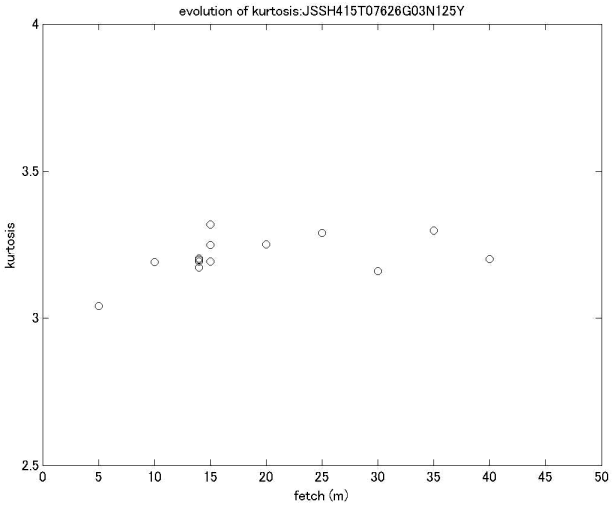

Figure 13: Evolution of Kurtosis with fetch. γ=3.0, n=125

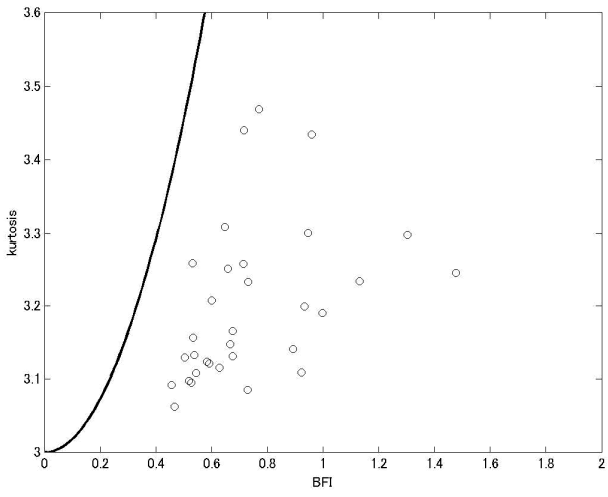

Figure 14: Kurtosis plotted against BFI Curved line corresponds to (13)

According to (14), the BFI in our experiment ranged between $0.4 < BFI < 1.4$. The estimated kurtosis is compared against the estimated BFI in Figure 14. The solid line corresponds to (13) which tends to show much larger value than the observation. There is some arbitrariness in the estimation of the BFI from the spectrum that may account for this discrepancy, but the overall scatter of the observation clearly suggests the significance of the directionality and the breaking dissipation not considered in the derivation of (13). The breaking dissipation, as described in section 4.1 imposes an upper limit to the maximum attainable wave height and correspondingly affects the estimation of the kurtosis; kurtosis can take a much higher values based on NLS (not described in this paper, see 9th Wave workshop abstract).

Next, the selected cases that do not involve energetic breakers will be analyzed to isolate the effects of each parameter on the value of the kurtosis. The frequency bandwidth of the spectrum is defined as

$$\delta f^2 = \frac{\int f^2 S(f) df}{m_0} \qquad (15)$$

and was estimated at the initial stage (fetch 14-15 m). In Figure 15, kurtosis at fetch 35-40 m for the Hwang directional distribution cases are plotted against the frequency bandwidth (γ varied between 1 and 30). The two symbols (blue and black) are for Hs around 5 cm (ak=0.08) and 4 cm (ak=0.06) cases respectively. For both cases, the value of the kurtosis reduces as the frequency bandwidth increases, and beyond $\delta f = 1.6$ or equivalently $\gamma = 5$ of the JONSWAP spectrum, the kurtosis remains unchanged. The BFI of the narrowest case shown here is about 0.7, and so, according to (13) the kurtosis should be about 3.8, which is much higher than the experimental result. The cases presented in Figure 15 are for Hwang directional distribution, whose approximate directional spreading is about 15 degrees. We next observe the kurtosis as a function of directionality.

For JONSWAP peakedness parameter γ=3.0, the kurtosis at its developed stage is plotted against directional spreading (circles). The kurtosis decreases with directionality and above 7 degrees or so, which corresponds to n=25 of the Mitsuyasu distribution (5), the value remains constant, despite the same BFI. The limit of 7 degrees is much narrower than the Alber and Saffman limit of the instability which is about 17 degrees. The experimental result indicates much narrower directional spreading for the non-resonant interaction to be active.

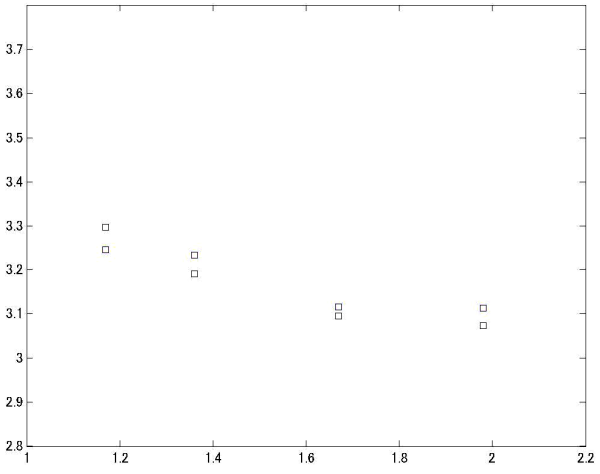

Figure 15: Kurtosis plotted against the frequency bandwidth.

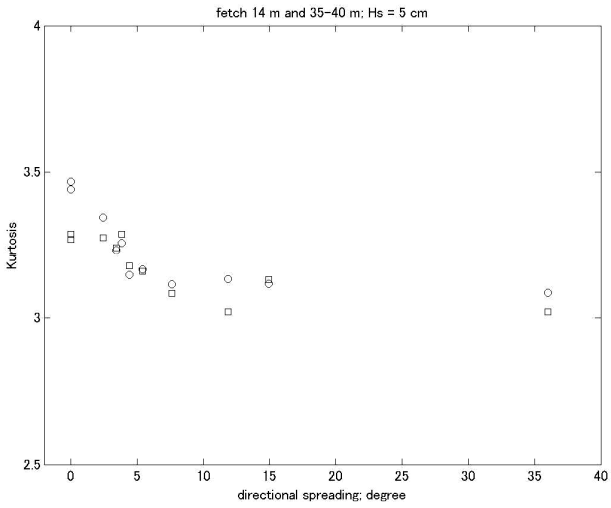

Figure 16: Kurtosis plotted against directional spreading (degrees); circle 35-40 m, square 14-15 m

In Figure 16, the initial values of the kurtosis are plotted together (square). For narrow directional spreading, the value tends to be lower than the kurtosis at the developed stage (circle), but for large directional spreading, the values are about the same. Therefore, for the cases whose directionality is larger than 10 degrees or so, the kurtosis remains more or less constant, which suggest that the non-resonant interaction (i.e. the second term of the right hand side of (12)) is negligible. What accounts for this slight increase of the Kurtosis is the third term and the finding suggests that the wave shape is distorted immediately before the non-resonant interaction takes place. The existence of the bound wave, therefore, seems to be important, for directional spreading over 10 degrees or so. It seems then, that for a typical ocean wave, the increase of the Kurtosis is mostly due to existence of the bound wave.

5. DISCUSSION

One of the most important and robust feature of the ocean wave is the increase of wavelength and amplitude as it grows with fetch and duration. Primary driving mechanism for this spectral downshifting is postulated as due to the nonlinear energy transfer by resonance wave-wave interaction. The nonlinear source term is an integral of infinite combinations of quartet of waves that satisfies the resonance condition. Hasselman et al. (1985) have shown that this nonlinear energy transfer can be approximated without loss of principle feature by a single combination of waves. The approximate angle of the most effective wave combination is about 27 degrees. Therefore, the wave spectrum tends to broaden or narrow if the directional spreading is less or more than the equilibrium spectrum; i.e. the directional wave self-stabilizes when they are perturbed (Young and Van Vledder 1993). However, when the waves become sufficiently narrow, narrow enough that the nonlinear transfer becomes ineffective, the waves transition to a swell. This is the conventional view.

The experimental findings in this study provide us a different perspective. When wave spectrum becomes sufficiently narrow, non-resonant interaction becomes the main driving mechanism for its evolution. Spectral shape changes accordingly, and when breaking dissipation is absent, the time averaged wave spectrum maintains its original shape. However, when breaking dissipation is present, the spectral change becomes irreversible and the spectral peak permanently shifts to lower frequency due to the imbalance of the wave energy and momentum. Therefore, although the energy transfers due to resonant wave-wave interaction is weak, the combination of non-resonant interaction and breaking dissipation results in a downshifting of the spectrum. As a result, wave statistics deviate from the conventional one and freak waves occur.

In order for the non-resonant interaction to be effective, we have shown that both the frequency bandwidth and the directional spreading need to be sufficiently narrow; in terms of the JONSWAP peakedness parameter $\gamma>5.0$ and of the Mitsuyasu distribution (5) $n>25$. How likely is this condition realized in the real ocean? We will now look into a coupled wave-current model output near Japan. The model was established based on an improved third generation wave model coupled with a realistic ocean prediction model JCOPE (Tamura et al., R1 Nov.16 10th Wave Workshop). The simulated one month (October of 2004) includes two passages of a sizable typhoon. An example distribution of the frequency bandwidth and the directional spreading is shown in Figure 17 for the case a typhoon is approaching Japan from South-Western end of the displayed domain. The region that satisfies the condition ($\gamma>5.0$ and $n>25$) are circled for clarity. Evidently, the region is highly restricted in the case of frequency distribution (left Figure 17); they are located at the front of the developing wind-sea region where the significant wave height is increasing (not shown). Similarly, the directional distribution tends to be narrow at the frontal region, but the distribution is much wider (right Figure 17). In addition, a broad area with relatively small wave energy exists in the Sea of Japan, suggestive of

a swell dominated region. These regions overlap in a restricted area, and according to the experimental finding, that is the dangerous sea where the freak wave might occur. Since there is no sea-truth available in the suggested dangerous seas, an observation is needed to prove the hypothesis. The overall distribution of the frequency bandwidth and the directional spreading was obtained from the 1-month simulation output (Figure 18). The histograms seem to have different character. The distribution of the frequency bandwidth is peaked around γ=2.0 and drops rapidly for larger γ; the occurrence of instability is quite rare. On the other hand, the distribution of the directionality is double peaked, the first peak around n=25 and the second peak around n=3. The latter is a typical wind-sea where as the former corresponds to either swell transition or swell-wind-sea mixed region. The region of possible instability (n>25), therefore, is much larger than the region constrained by the frequency spreading. It should be noted here that the actual spectral shape is highly complicated, and so a closer look at the spectral shape is needed. Finally, the downshifting due to breaking dissipation is not included in the numerical model and so the accuracy of the prediction should be verified against observation.

ACKNOWLEDGEMENT

The first author would like to thank Mr. Itakura for his assistance in conducting the experiment. The Benjamin-Feir instability experiments were conducted by the students Mr. Kameoka and Mr. Kinoshita who have completed their master's and bachelor's thesis. A part of the study was supported by grant-in-aid program of the MEXT. The manuscript is intended to be submitted for a journal publication with some revision, and therefore, a part of the text as well as figures will be reproduced there.

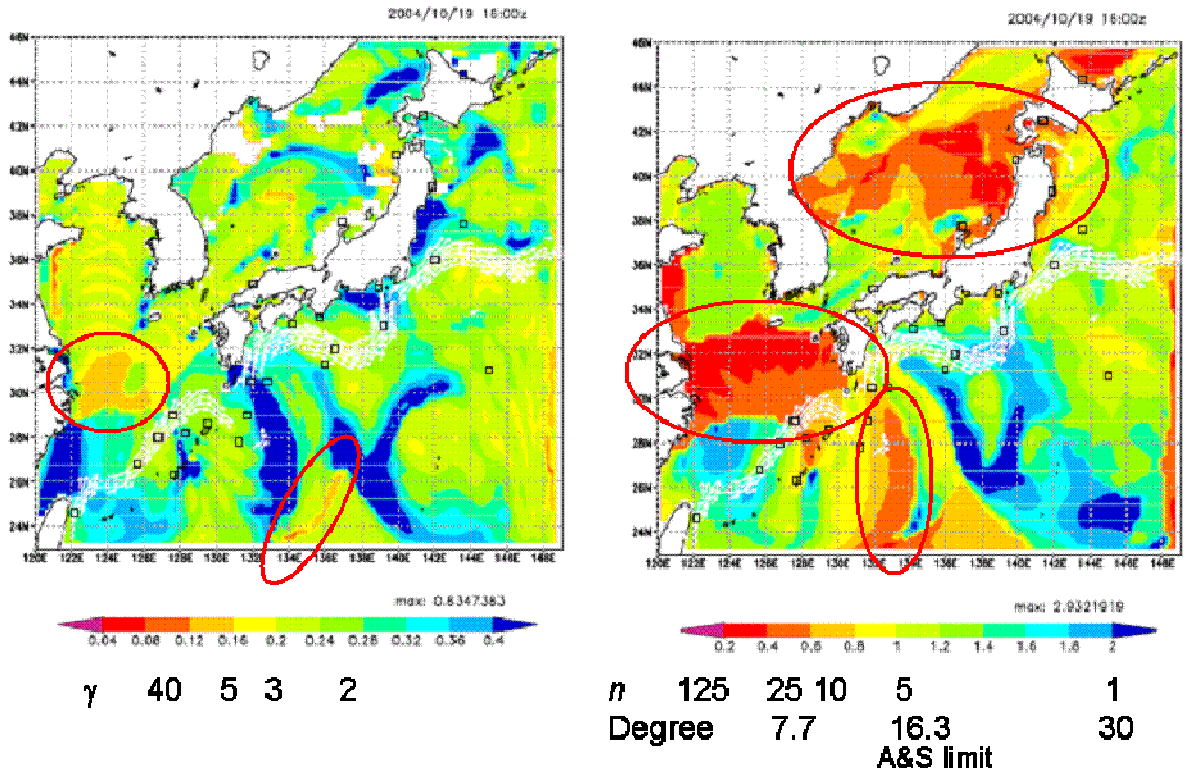

Figure 17: Distribution of frequency spreading (left) and directional spreading (right) from the couple wave-current model.

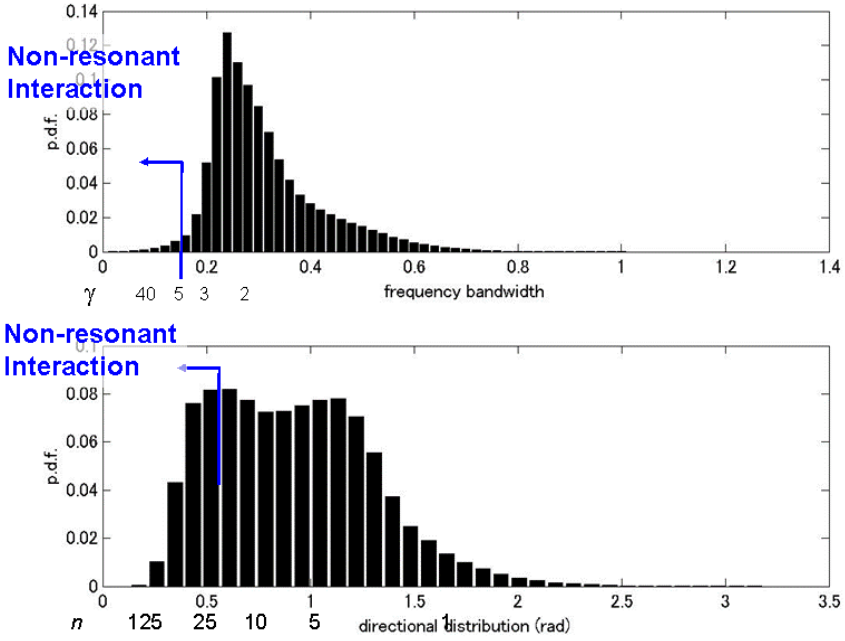

Figure 18: Histogram of frequency bandwidth (top) and directional distribution (bottom) from a month of hindcast wind-sea near Japan.

REFERENCES

Alber, I. and P. Saffman, "Stability of random nonlinear deepwater waves with finite bandwidth spectra", Tech Rep. 32326-6035-RU-00, TRW Defense and Space System Group

Benjamin, T.B. and J.E. Feir, 1967, The disintegration of wave trains on deep water Part 1. Theory, J. Fluid Mech. 27, 417-

Dysthe, K. H. Socquet-Juglard, K. Trulsen, H. Krogstad, and J. Liu, "Freak" waves and large-scale simulations of surface gravity waves, Rogue Waves 2004, edited by M. Olagnon and M. Prevosto

Hasselmann, S., K. Hasselmann, J. H. Allender and T. P. Barnett, 1985: Computations and parameterizations of the nonlinear energy transfer in a gravity-wave spectrum. Part II: Parameterizations of the nonlinear energy transfer for application in wave models. *J. Phys. Oceanogr.*, 15, 1378-1391.

Hwang, P. A. and D. W. Wang, "Directional distribution and mean slopes in the equilibrium and saturation ranges of wave spectrum", J. Phys. Oceanogr. 31, 2001, 1346-1360

Janssen, P.A.E.M., 2003, Nonlinear four-wave interactions and freak waves, J. Phys. Oceanogr., 33, 863-884

Janssen, P.A.E.M. and Bidlot, 2003, New wave parameters to characterize Freak Wave Conditions. ECMWF Memo, Research Department, R60.9.PJ/0387, ECMWF, Reading, U.K.

Lamont-Smith, T., J. Fuchs and M. P. Tulin, 2003, Radar Investigation of the Structure of Wind Waves, J. Oceanogr., 59(1), 49-63

Melville, K., 1982, The instability and breaking of deep-water wave, J. Fluid Mech., 115, 165-185

Mori, N. and P.A.E.M. Janssen, 2006, On Kurtosis and occurrence probability of Freak Waves, J. Phys. Oceanogr., 36(7), 1471-1483

Onorato, M., Osborne, A.R. and M. Serio, 2002, Extreme wave events in directional, random oceanic sea states, Physics of Fluids, 14 (4), 25-28

Onorato, M., A.R. Osborne, M. Serio, L. Cavaleri, C. Brandini, C.T. Stansberg, 2004, Observation of strongly non-Gaussian statistics for random sea surface gravity waves in wave flume experiments, Phys. Review E, 70, 067302

Onorato, M., Osborne, A.R. and M. Serio, 2005, On deviations from Gaussian statistics for surface

gravity waves, preprint
Poulter, E. M., M. J. Smith, J. A. McGregor, Microwave backscatter from the sea surface: Bragg scattering by short gravity waves, J. Geophys. Res., 99(C4), 7929-7944, 10.1029/93JC03562, 1994.
Soquet-Juglard, H., K. Dysthe, K. Trulsen, H.E. Krogstat, J. Liu, 2005, Probability distribution of surface gravity waves during spectral changes, J. Fluid Mech., 542, 195-216
Su M.-Y, Green A. W., 1984, Coupled Two-dimensional and 3-dimensional instabilities of surface gravity-waves, Physics of fluids, 27 (11): 2595-2597
Tanaka, M., 1990, Maximum amplitude of modulated wave train, *Wave Motion*, 12, 559-568
Tulin M.P., "Breaking waves in the ocean and around ships", Twenty-third symposium on Naval Hydrodynamics, 2001
Tulin, M.P. and T. Waseda, 1999, Laboratory observations of wave group evolution, including breaking effects, J. Fluid Mech., 378, 197-
Waseda, T., 2006, Experimental investigation and applications of the modulational wave train、Online Extended Abstract : Workshop on Rogue Wave, *http://www.icms.org.uk/meetings/2005/roguewaves/index.html*
Waseda, T. and M. P. Tulin (1999), 'Experimental study of the stability of deep-water wave trains including wind effects', *J. Fluid Mech., 401,* 55-84
Waseda, T, C.-K. Rheem, J. Sawamura, T. Yuhara, T. Kinoshita, K. Tanizawa and H. Tomita, 2005, Extreme Wave Generation in Laboratory Wave Tank, the Proceedings of the Fifteenth International Offshore and polar engineering conference, Vol. III, 1-9
Young, I.R. and G.Ph. Van Vledder, 1993: A review of the central role of nonlinear interactions in wind - wave evolution, *Trans. of the Roy. Soc. London*, 342, 505-524.
Yuen, H., and B. Lake, 1982, Nonlinear dynamics of deep-water gravity waves, Adv. Appl. Mech., 22, 67-229
Zakharov, V., 1968, Stability of periodic waves of finite amplitude on the surface of deep fluid, J. Appl. Mech. Tech. Phys. (English transl.), 2, 190-194